

#### **OPEN ACCESS**

EDITED BY

Enrique Soto,

Meritorious Autonomous University of Puebla,

REVIEWED BY

Elias Manjarrez,

Meritorious Autonomous University of Puebla,

Mexico

Adriana Pliego

Universidad Autónoma del Estado de México, Mexico

\*CORRESPONDENCE

Seo Yoon Park,

pgy0614@hanmail.net

<sup>1</sup>These authors have contributed equally to this work and share first authorship

RECEIVED 19 August 2025 REVISED 01 November 2025 ACCEPTED 03 November 2025 PUBLISHED 26 November 2025

#### CITATION

Yun SH, Yeo SS and Park SY (2025) Modulation of VR-HMD-induced cybersickness using cathodal transcranial direct current stimulation: a functional near-infrared spectroscopy study. *Front. Virtual Real.* 6:1688562. doi: 10.3389/frvir.2025.1688562

#### COPYRIGHT

© 2025 Yun, Yeo and Park. This is an openaccess article distributed under the terms of the Creative Commons Attribution License (CC BY). The use, distribution or reproduction in other forums is permitted, provided the original author(s) and the copyright owner(s) are credited and that the original publication in this journal is cited, in accordance with accepted academic practice. No use, distribution or reproduction is permitted which does not comply with these terms.

# Modulation of VR-HMD-induced cybersickness using cathodal transcranial direct current stimulation: a functional near-infrared spectroscopy study

Seong Ho Yun<sup>1†</sup>, Sang Seok Yeo<sup>2†</sup> and Seo Yoon Park<sup>3</sup>\*

<sup>1</sup>Department of Public Health Sciences, Graduate School, Dankook University, Cheonan, Republic of Korea, <sup>2</sup>Department of Physical Therapy, College of Health and Welfare Sciences, Dankook University, Cheonan, Republic of Korea, <sup>3</sup>Department of Physical Therapy, College of Health and Welfare, Woosuk University, Wanju, Republic of Korea

Virtual reality head-mounted displays (VR-HMDs) can induce cybersickness symptoms, including nausea, dizziness, and disorientation, due to sensory conflicts between visual and vestibular inputs. This study investigated the effects of cathodal transcranial direct current stimulation (tDCS) on cybersickness symptoms and cortical activity during VR experiences. Twenty healthy adults were randomly assigned to either the cathodal tDCS group (n = 10) or the sham stimulation group (n = 10). Participants underwent VR rollercoaster exposure while cortical activity was measured using functional near-infrared spectroscopy (fNIRS) before and after 20 min of 2 mA cathodal tDCS applied over the right temporoparietal junction (TPJ). Cybersickness symptoms were assessed using the Simulator Sickness Questionnaire (SSQ). Results showed that cathodal tDCS significantly reduced nausea-related cybersickness symptoms compared to sham stimulation (p < 0.05). fNIRS analysis revealed decreased oxyhemoglobin concentrations in the bilateral superior parietal lobule and angular gyrus following cathodal tDCS, indicating reduced cortical activity in these regions. Betweengroup comparisons confirmed greater reductions in cortical activity in the right TPJ regions for the cathodal group than for the sham group. These findings suggest that cathodal tDCS over the right TPJ can effectively mitigate cybersickness by modulating cortical activity in brain regions associated with multisensory integration and vestibular processing.

KEYWORDS

cybersickness, transcranial direct current stimulation, virtual reality, functional near-infrared spectroscopy, temporoparietal junction

#### Introduction

A virtual reality (VR) head-mounted display (HMD) is a form of immersive VR that positions two small screens in front of each eye, completely blocking the physical world, including the user's body, and allows the user to turn their head to examine their surroundings (Bailey and Bailenson, 2017). Because VR-HMD aims to achieve immersive effects simply and inexpensively, immersion and presence play a crucial role (Diemer et al., 2015). However, immersive VR can cause symptoms similar to general motion sickness (MS), such as nausea, dizziness, and headaches, known as cybersickness (Schmäl, 2013; Sugiura et al., 2017). In this context, dizziness refers to a general sense of

unsteadiness, lightheadedness, or spatial disorientation rather than true rotational vertigo, which is characterized by a specific illusion of spinning or movement (Bisdorff, 2014; LaViola et al., 2000). Cybersickness is explained by the sensory conflict theory, where discrepancies between visual and vestibular inputs in VR environments cause dysfunction in the "vestibular network." This network, encompassing autonomic, sensorimotor, and cognitive regions, receives conflicting signals during VR exposure, leading to symptoms such as nausea and disorientation. Generally, cybersickness is assessed using self-report measures after VR experiences. However, this method can be affected by temporal dynamics and recall bias, so the results should be interpreted with caution (Young et al., 2007).

Neuroimaging studies have identified several brain regions that are critical to the integration of vestibular and visual inputs during sensorimotor conflicts. These include the parieto-insular vestibular cortex (PIVC), supramarginal gyrus (SMG), superior temporal gyrus (STG), temporoparietal junction (TPJ), and angular gyrus (AG) (Arshad et al., 2015). The TPJ plays a crucial role in multimodal sensory integration, spatial cognition, and self-body consciousness. It is involved not only in maintaining balance during sensory conflicts but also in continuously processing and integrating vestibular, visual, and proprioceptive information to create a coherent representation of the body in space. This region is particularly important in VR environments where sensory inputs may be incongruent (Arshad et al., 2015; Jöbsis, 1977). Functional near-infrared spectroscopy (fNIRS) has been reported to offer several advantages over other neuroimaging techniques for studying cybersickness. Compared to functional magnetic resonance imaging (fMRI), fNIRS has advantages such as portability, cost-effectiveness, better temporal spatial resolution. and higher resolution electroencephalography (EEG). It is, therefore, ideal for detecting rapid changes in cortical activity associated with the onset of cybersickness (Ayaz et al., 2019). fNIRS studies have cybersickness reported that experiencing oxyhemoglobin (HbO) concentrations in parietotemporal regions, and HbO concentrations are positively correlated with nausea and motion sickness symptoms. Moreover, fNIRS has shown promise in detecting cognitive demands and emotional arousal, making it particularly suitable for investigating the complex neural processes underlying cybersickness (Jöbsis, 1977; Yamamura et al., 2020).

Transcranial direct current stimulation (tDCS) represents a non-invasive approach to modulate neuronal activity within specific brain areas through the application of a low-intensity direct current (Filmer et al., 2014; Flöel, 2014). The tDCS applied over the TPJ has shown positive effects in alleviating cybersickness and improving postural stability. tDCS could be applied in two primary modes: anodal and cathodal. Anodal tDCS typically increases cortical excitability, while cathodal tDCS tends to decrease it. The efficacy and duration of tDCS effects depend critically on stimulation parameters, particularly current intensity and duration. Although some preliminary studies have used lower intensities (e.g., 1.5 mA) for shorter durations (e.g., 15 min) (Li et al., 2020), evidence-based guidelines recommend 2 mA for 20 min as the standard protocol for cathodal tDCS to achieve robust cortical

modulation with sustained aftereffects (Lefaucheur et al., 2017; Nitsche et al., 2008). This protocol produces consistent neurophysiological effects and induces cortical excitability changes lasting 60-90 min post-stimulation (Nitsche and Paulus, 2001). Given that our study aimed to detect cortical activity changes using fNIRS during VR exposure, we opted for this established protocol to maximize the likelihood of observing significant cortical modulation and therapeutic effects on cybersickness. However, there is a lack of research on cathodal tDCS for dizziness and vestibular dysfunction. Therefore, modulating cortical excitability in the TPJ associated with multisensory and vestibular processing may prove beneficial in alleviating cybersickness symptoms. In their studies, Takeuchi et al. (2018) investigated the effects of anodal tDCS on cybersickness induced by a VR rollercoaster. As the results show, cybersickness, including oculomotor dysfunction after VR exposure, was related to anodal tDCS.

Therefore, the purpose of this study is to investigate the effects of applying cathodal tDCS on changes in cortical activation and to determine its effectiveness in reducing actual cybersickness.

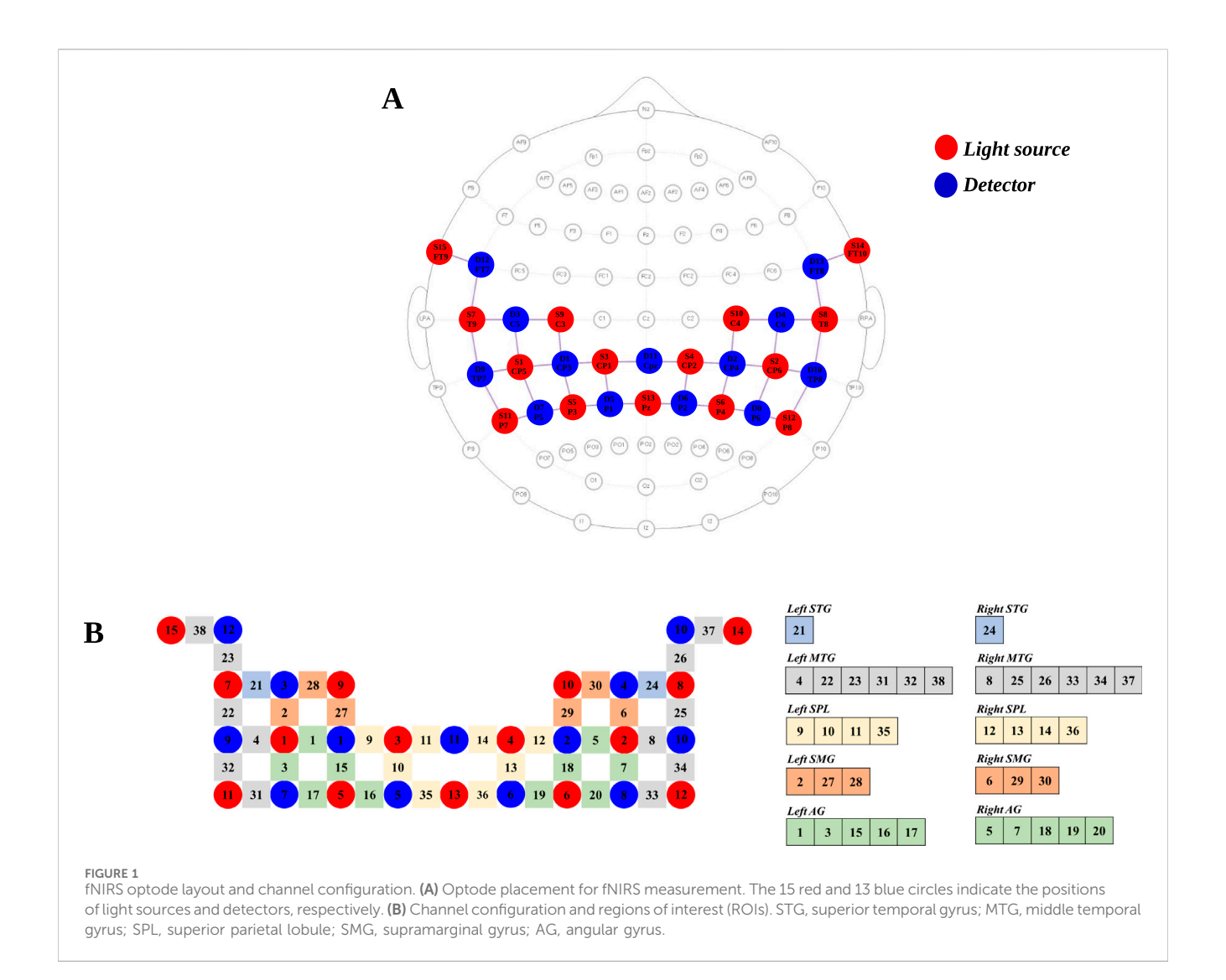
#### Materials and methods

## **Participants**

A total of 20 healthy adults with no musculoskeletal, neurological, or psychiatric disorders were recruited for this study. Participants who had prior exposure to externally stimulated experiments of the tDCS or transcranial magnetic stimulation (TMS) were excluded. The experiments were conducted in accordance with the principles outlined in the Declaration of Helsinki. The study protocol was approved by the Institutional Review Board of Dankook University (DKU 2023-01-016-001).

#### Transcranial direct current stimulation

tDCS was delivered using a direct current stimulator (ActivaDose, ActivaTek Inc., Salt Lake City, United States), with a pair of saline-soaked surface sponge electrodes (25 cm<sup>2</sup>). The electrodes were positioned according to the international 10-20 system and secured using a strap (Caputron, New York, United States). In the cathodal group, the cathodal electrode was attached to CP6, corresponding to the right TPJ. The anodal electrode was placed over Cz, a common reference position in tDCS studies that minimizes confounding effects on the target stimulation site while maintaining a stable current flow (Cesari et al., 2024). This midline vertex position has been widely used in previous tDCS studies targeting the TPJ to ensure that the primary neuromodulatory effects occur at the cathodal electrode site. Current was provided for 20 min at an intensity of 2 mA and ramped up or down over the first and last 30 s of stimulation. In the sham group, electrodes were placed in the same positions as the cathodal group; however, the current was delivered only for the initial and last 30 s (Lefaucheur et al., 2017). Electrode impedance was maintained below 10 k $\Omega$  throughout the stimulation session



by ensuring proper saline saturation of the sponge electrodes (Llorens et al., 2021).

#### Functional near-infrared spectroscopy

fNIRS data were measured using continuous wave NIRSport2 (NIRx Medical Technologies LLC, Berlin, Germany). The sampling rate was set to 12.52 Hz. Optodes were attached to the cap in accordance with the international 10–20 system using NIRSite software (NIRx Medical Technologies, LLC, LA, United States) and the fNIRS Optodes' Location Decider toolbox. A total of 15 emitters and 12 detectors were used to measure optical light intensity at two different wavelengths (760 m and 850 m), resulting in a total of 38 channels. The regions of interest (ROIs) were bilateral superior temporal gyrus, middle temporal gyrus, superior parietal lobule, supramarginal gyrus, and angular gyrus because the temporoparietal junction was associated with vestibular and proprioception processing and multisensory integration (Frank and Greenlee, 2018; Dieterich and Brandt, 2008) (Figure 1).

# Simulator Sickness Questionnaire

Cybersickness symptoms were assessed using the Simulator Sickness Questionnaire (SSQ). The SSQ is a self-report instrument designed to measure symptoms associated with simulator sickness (Kennedy et al., 1993). It comprises 16 items related to cybersickness symptoms, namely, general discomfort, fatigue, headache, eyestrain, difficulty focusing, increased salivation, sweating, nausea, difficulty concentrating, fullness of head, blurred vision, dizziness with eyes open, dizziness with eyes closed, vertigo, stomach awareness, and burping. Each item is rated on a four-point Likert scale (0 = none, 1 = mild, 2 = moderate, and 3 = severe). A total SSQ score and three subscale scores are calculated as follows: nausea (reflecting symptoms such as stomach discomfort, increased salivation, and nausea), oculomotor discomfort (reflecting visual strain symptoms including eyestrain, difficulty focusing, blurred vision, and headache), and disorientation (reflecting dizziness and vertigo). The SSQ has demonstrated high internal consistency with a Cronbach's alpha of 0.868 (Bouchard et al., 2007).

TABLE 1 Comparison of SSQ scores within/between groups.

	s within between groups.			
	Cathodal	Sham	<i>p</i> -value	
Total SSQ				
Pre	70.69 ± 60.16	69.40 ± 65.27	0.010*	
Post	55.35 ± 64.77	86.02 ± 61.31		
Difference	$-23.19 \pm 31.33$	16.62 ± 22.45		
<i>p</i> -value	0.089	0.057		
Nausea				
Pre	41.02 ± 59.50	56.18 ± 58.51	<0.001*	
Post	33.39 ± 60.21	75.26 ± 61.91		
Difference	$-10.49 \pm 12.27$	19.08 ± 14.31		
<i>p</i> -value	0.022*	0.004		
Oculomotor				
Pre	54.58 ± 45.48	47.16 ± 43.67	0.059	
Post	45.48 ± 41.82	59.80 ± 36.83		
Difference	$-15.92 \pm 28.24$	12.63 ± 19.33		
p-value	0.305	0.086		
Disorientation				
Pre	100.22 ± 77.31	89.71 ± 85.27	0.085	
Post	73.77 ± 81.18	100.53 ± 78.37		
Difference	-41.76 ± 53.31	10.83 ± 42.78		
<i>p</i> -value	0.100	0.469		

Values represent mean ( $\pm$  standard deviation); SSQ, Simulator Sickness Questionnaire.  $^*p < 0.05$ .

#### **Procedure**

This study implemented a randomized, single-blind, and shamcontrolled design to investigate the effects of tDCS on cybersickness symptoms and cortical activity. All participants were randomly allocated to either the cathodal group (n = 10) or the sham group (n = 10). In the pre-tDCS test, participants were equipped with an HMD VR system (Oculus Quest 2, Meta, United States) and fNIRS devices. All trials were conducted in a quiet, controlled laboratory environment to minimize external distractions. Participants performed the VR task in a standing position. Before starting the experiment, participants were informed that the VR scene could cause temporary symptoms such as dizziness or nausea and that they could stop the experiment at any time if necessary. The experimental session consisted of a three-block paradigm. Each block included a 30-s rest phase, a 120-s task phase, and a 30-s recovery phase, resulting in a total fNIRS recording duration of 450 s (7.5 min). Although our three-block experimental design was relatively short compared to that in some neuroimaging studies, we adopted this design due to the burden of cybersickness on participants. There is currently no gold standard for the number of blocks required to reduce the variability of hemodynamic responses. Nevertheless, previous studies have demonstrated that using at least three blocks enables adequate averaging of hemodynamic changes and reduces anticipatory contributions (Herold et al., 2017). Moreover, a previous fNIRS study investigating hemodynamic responses during autonomous driving used a 120-s task block, with a 30-s rest period (Hidalgo-Muñoz et al., 2019). During the resting phase, participants were instructed to fixate on a cross in the center of a black screen. During the task phase, participants observed the same virtual rollercoaster scene three times, each lasting 120 s. The duration of the VR exposure was determined based on previous studies investigating cybersickness. The virtual rollercoaster scene was selected to induce cybersickness through sensory mismatch between visual motion cues (rapid movements and rotations in the virtual environment) and vestibular/proprioceptive inputs, rather than solely through high-speed visual motion. This discrepancy between the visual perception of self-motion and the absence of corresponding physical movement creates the sensory conflict that is central to cybersickness. The severity of cybersickness symptoms was assessed using the SSQ after the experiment. Then, cathodal and sham groups received real tDCS and sham tDCS, respectively, for 20 min. The post-tDCS test was conducted in the same way as the pre-tDCS test.

#### Data analysis

NIRS-Lab ver 2019.04 (NIRx Medical Technologies LLC, Berlin, Germany) was used to analyze fNIRS data. The coefficient of variation (CV = standard deviation/mean) with a level of 15% or less was regarded as adequate for the quality of each channel. During data pre-processing, discontinuities and spike artifacts were removed (Zhang et al., 2018; Pfeifer et al., 2018). Then, the data were filtered using a 0.001–0.20 Hz bandpass filter with a 15% roll width to eliminate the effects of heartbeat and respiration (Zhang et al., 2018; Azhari et al., 2021). The modified Beer–Lambert law was used to convert optical density to HbO and deoxy-hemoglobin (HbR) concentrations (Cope

TABLE 2 Significant channels of HbO in the group analysis (p < 0.01).

	Channel	t-value	<i>p</i> -value
Cathodal pre			
Left superior parietal lobule	9	3.01	0.007
	10	3.39	0.004
Right superior parietal lobule	13	4.50	< 0.001
Right middle temporal gyrus	8	4.28	0.001
Right angular gyrus	5	3.05	0.007
	18	3.91	<0.001
	19	3.12	0.006
	6	3.35	0.004
	29	3.44	0.004
	30	3.08	0.007
Cathodal post			
Left angular gyrus	15	-3.47	0.004
	16	-3.58	0.003
	17	-3.39	0.004
Right superior parietal lobule	14	-4.41	< 0.001
Right angular gyrus	19	-3.11	0.006
Sham pre			
Left superior parietal lobule	10	3.84	0.002
Left middle temporal gyrus	22	3.16	0.007
	32	3.04	0.008
Right middle temporal gyrus	25	3.31	0.005
	26	4.09	0.002
Sham post			
Left angular gyrus	3	-3.20	0.006

Values represent mean (± standard deviation); HbO, oxyhemoglobin.

and Delpy, 1988; Baker et al., 2014). We focused on HbO for further analysis because it has a higher signal-to-noise ratio and greater reliability than HbR.

For topographical analysis, we used the Statistical Parameter Mapping NIRS-SPM (SPM 8) tool executed in the NIRS-lab (version 2019.4). The general linear model (GLM), with a canonical hemodynamic response curve, was used to analyze the significant taskrelated cortical activation, separately for HbO, for each individual. At the individual level, an SPM-1 within-subject analysis was performed to estimate the degree of activation in each channel with respect to the resting condition. In SPM-1 analysis, a hemodynamic response function (HRF) was considered, and pre-whitening was omitted. HRF was plotted against a time axis using a convolution design matrix, where each point of the matrix was checked. This was followed by the application of a discrete cosine transform (DCT) temporal parameter with a high-pass period cut-off of 128 s. A Gaussian Full Width at Half Maximum (FWHM) 4 model was applied, and for each participant, GLMs were obtained based on the HbO signals. The beta coefficient derived from the GLM represents the amplitude of the hemodynamic response and quantifies the intensity of cortical activation (Perpetuini et al., 2022). Each channel contrast between the task and the resting condition was evaluated using a 1-sample t-test. For group analysis of the cortical activity, SPM-2 between-subject analysis was performed (statistical significance level was <0.01).

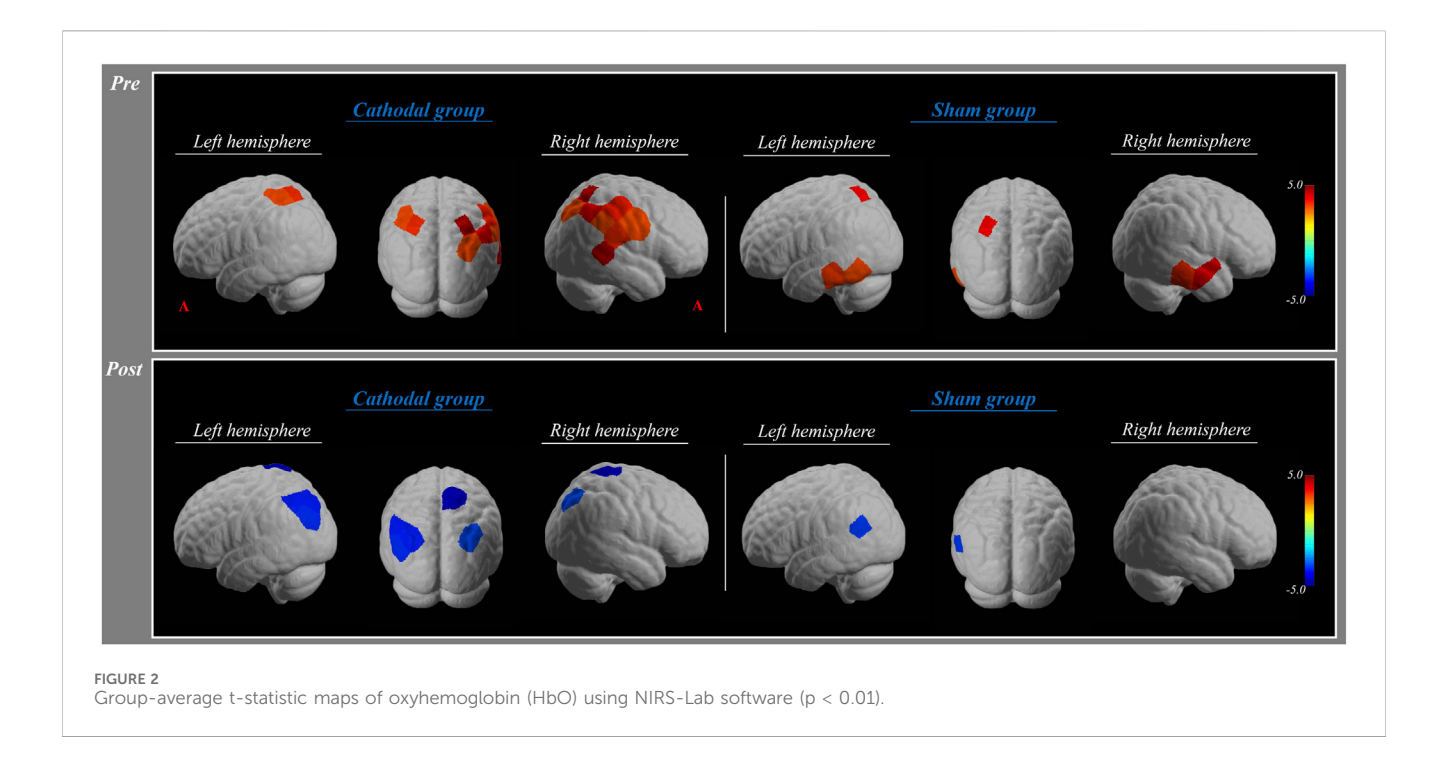
The beta coefficient and SSQ scores were analyzed using SPSS software (version 24.0; SPSS, Chicago, IL, United States). A paired t-test was performed to determine the differences in the beta coefficient of HbO and SSQ scores between the pre- and post-test in the cathodal and sham groups. The independent t-test was conducted to analyze the differences in the beta coefficient of HbO and SSQ scores between groups. Null hypotheses of no difference were rejected if *p*-values were <0.05.

#### Results

## Simulator Sickness Questionnaire

Table 1 shows the SSQ scores in the cathodal and sham groups. There was no significant difference in the total SSQ, nausea,

<sup>\*</sup>p < 0.01



oculomotor, and disorientation scores in the pre-test between groups (p > 0.05). In the within-group comparison, the nausea score in the cathodal group was significantly decreased after cathodal tDCS (p < 0.05). The total SSQ, oculomotor, and disorientation scores in the cathodal group were not significantly different between the pre- and post-tests (p > 0.05). In the sham group, there were no significant differences in the total SSQ, nausea, oculomotor, and disorientation scores between the pre- and post-tests.

In the between-group comparison, the nausea score in the cathodal group significantly decreased compared to that in the sham group (p < 0.05). Differences in the total SSQ, oculomotor, and disorientation scores were not significant between groups (p > 0.05).

#### Group analysis of HbO values

In the pre-test, the HbO values in the cathodal group showed significant activation in the bilateral superior parietal lobule, right middle temporal gyrus, and angular gyrus (p < 0.01). There was a significant activation in the bilateral middle temporal gyrus and left superior parietal lobule in the sham group (p < 0.01) (Table 2; Figure 2).

In the post-test, the HbO values in the cathodal group revealed significant deactivation in the bilateral angular gyrus, right superior parietal lobule, and middle temporal gyrus (p < 0.01). There was a significant deactivation in the left angular gyrus (p < 0.01) (Table 2; Figure 2).

#### Beta coefficient of HbO

In the pre-test, there were no significant differences in the beta coefficient of HbO in all regions of interest between groups (p >

0.05). In the within-group comparison, the beta coefficient of HbO in the bilateral superior parietal lobule and angular gyrus in the cathodal group was significantly decreased after cathodal tDCS (p < 0.05). In the sham group, there were no significant differences in the beta coefficient of HbO in all regions of interest between the pre- and post-tests (p > 0.05) (Table 3; Figure 3).

In the between-group comparison, the beta coefficient of HbO in the right superior parietal lobule and angular gyrus in the cathodal group significantly decreased compared to that in the sham group (p < 0.05) (Table 3; Figure 3).

# Discussion

The primary objective of this study was to examine the impact of cathodal tDCS on cybersickness symptoms and cortical activity during VR rollercoaster experiences in healthy adults. Cortical activity was assessed through hemodynamic response measurements using fNIRS. Our investigation yielded three principal findings: (1) participants in the cathodal tDCS group exhibited a significant reduction in nausea-related cybersickness symptoms compared to those in the sham group. This suggests that cathodal tDCS may have a mitigating effect on the nausea component of cybersickness. (2) Following cathodal tDCS administration, we observed a significant decrease in the beta coefficients of the bilateral superior parietal lobule and angular gyrus. This reduction in beta coefficients, which represent the relationship between the predictor variables and the response variable in our statistical model, indicates a decrease in cortical activity in these regions, as reflected by changes in HbO and deoxygenated hemoglobin concentrations. (3) The cathodal group demonstrated significantly greater changes in beta coefficients within the right superior parietal lobule and angular gyrus than

TABLE 3 Comparison of the beta coefficients of HbO within/between groups.

	Cathodal	Sham	<i>p</i> -value
Left superior temporal gyrus			
Pre	-0.00005 ± 0.00076	$-0.00013 \pm 0.00104$	0.509
Post	$-0.00021 \pm 0.00054$	$0.00009 \pm 0.00072$	
Difference	$-0.00016 \pm 0.00062$	$0.00023 \pm 0.00167$	
<i>p</i> -value	0.451	0.695	
Left middle temporal gyrus			
Pre	$0.00014 \pm 0.00042$	0.00028 ± 0.00041	0.147
Post	$0.00014 \pm 0.00041$	$-0.00004 \pm 0.00034$	
Difference	$0.00000 \pm 0.00043$	$-0.00032 \pm 0.00050$	
p-value	0.974	0.092	
Left superior parietal lobule			
Pre	0.00028 ± 0.00034	0.00023 ± 0.00035	0.096
Post	$-0.00017 \pm 0.00047$	0.00009 ± 0.00038	
Difference	$-0.00045 \pm 0.00039$	$-0.00013 \pm 0.00039$	
p-value	0.005*	0.332	
Left supramarginal gyrus			
Pre	0.00012 ± 0.00044	0.00026 ± 0.00048	0.221
Post	$0.00010 \pm 0.00057$	$-0.00006 \pm 0.00032$	
Difference	$-0.00028 \pm 0.00041$	$-0.00032 \pm 0.00060$	
p-value	0.836	0.143	
Left angular gyrus			
Pre	0.00016 ± 0.00040	0.00006 ± 0.00033	0.097
Post	$-0.00023 \pm 0.00036$	$-0.00011 \pm 0.00032$	
Difference	$-0.00040 \pm 0.00027$	$-0.00016 \pm 0.00031$	
<i>p</i> -value	0.001*	0.157	
Right superior temporal gyrus			
Pre	0.00006 ± 0.00066	0.00006 ± 0.00077	0.765
Post	$-0.00009 \pm 0.00040$	$0.00010 \pm 0.00059$	
Difference	$-0.00010 \pm 0.00078$	0.00003 ± 0.00112	
<i>p</i> -value	0.692	0.932	
Right middle temporal gyrus			
Pre	$0.00023 \pm 0.00044$	0.00028 ± 0.00046	0.460
Post	$0.00005 \pm 0.00053$	$0.00032 \pm 0.00043$	
Difference	$-0.00018 \pm 0.00057$	$0.00004 \pm 0.00066$	
<i>p</i> -value	0.348	0.876	
Right superior parietal lobule			
Pre	0.00037 ± 0.00045	0.00018 ± 0.00034	0.039*
Post	$-0.00010 \pm 0.00039$	0.00012 ± 0.00044	
Difference	$-0.00047 \pm 0.00033$	$-0.00007 \pm 0.00046$	
p-value	0.001*	0.677	
Right supramarginal gyrus			
Pre	$0.00042 \pm 0.00049$	0.00019 ± 0.00051	0.613
Post	$0.00009\pm0.00050$	$-0.00001 \pm 0.00043$	
Difference	$-0.00033 \pm 0.00049$	$-0.00021 \pm 0.00057$	
<i>p</i> -value	0.060	0.307	

(Continued on following page)

TABLE 3 (Continued) Comparison of the beta coefficients of HbO within/between groups.

		3 1	
	Cathodal	Sham	<i>p</i> -value
Right angular gyrus			
Pre	0.00022 ± 0.00040	0.00010 ± 0.00039	0.040*
Post	$-0.00010 \pm 0.00039$	$0.00006 \pm 0.00031$	
Difference	$-0.00033 \pm 0.00026$	$-0.00004 \pm 0.00031$	
<i>p</i> -value	0.003*	0.709	

Values represent mean (± standard deviation); HbO, oxyhemoglobin.

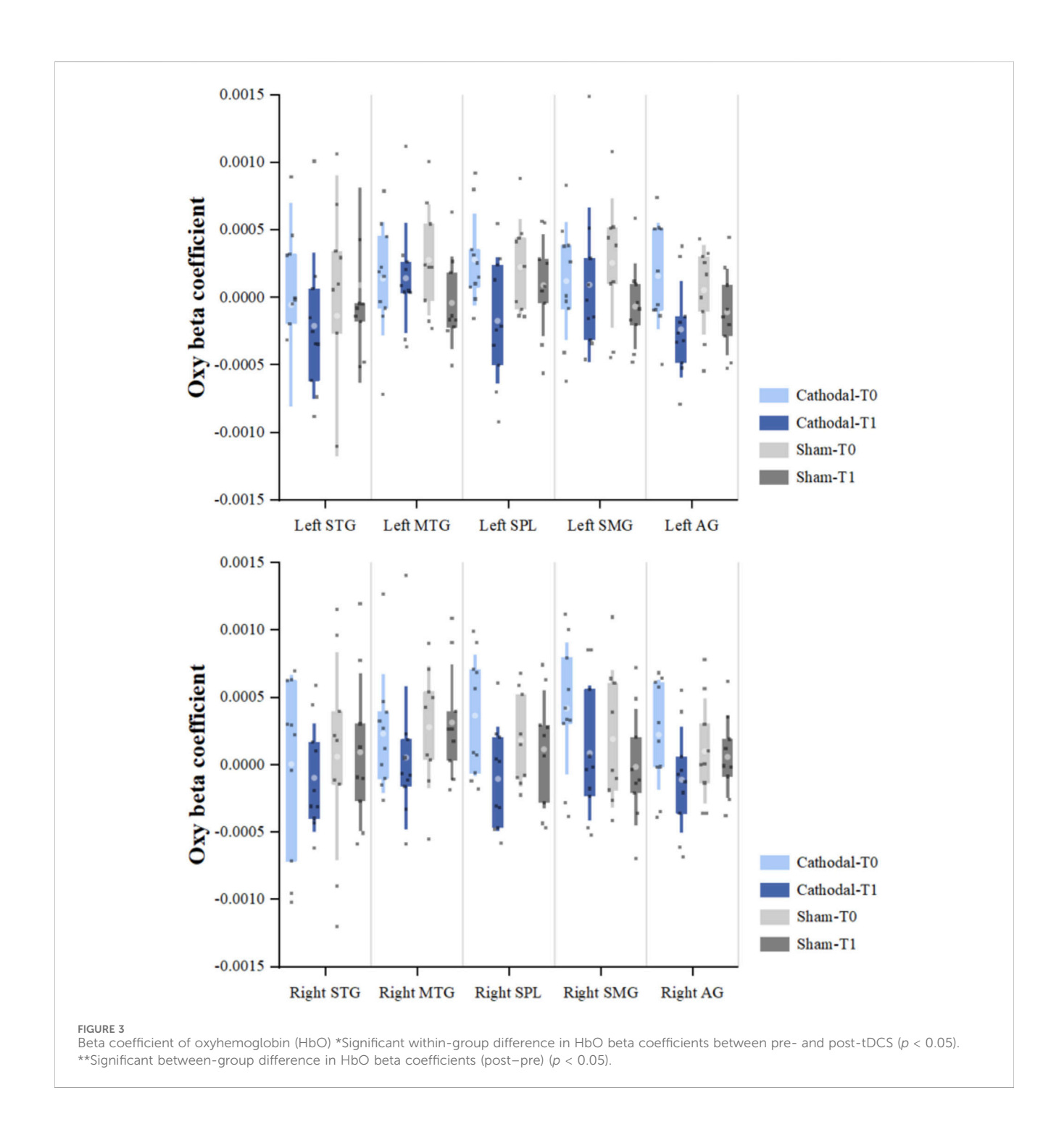
the sham group. This finding highlights the specific impact of cathodal tDCS on these cortical areas.

Importantly, negative coefficients for oxygenated and deoxygenated hemoglobin were interpreted as decreases in cortical activity. Collectively, these results suggest that cathodal tDCS may alleviate cybersickness symptoms by attenuating cortical activity in the temporoparietal junction, a region encompassing the superior parietal lobule and angular gyrus. As the target cortical region for tDCS, we selected the TPJ, implicated in self-motion perception and visual-vestibular integration (Pfeiffer et al., 2014). Our findings demonstrate that cathode placement over the right TPJ in the experimental group effectively modulated cortical activity, as evidenced by the observed differences in cybersickness symptoms and hemodynamic responses compared to those in the sham group. This modulation of TPJ activity through external brain stimulation directly affected the cybersickness experience in VR, supporting our initial hypothesis (Kheradmand and Winnick, 2017). Moreover, while tDCS targeting the TPJ modulates corticallevel multisensory integration, galvanic vestibular stimulation (GVS) acts peripherally by stimulating the vestibular afferents. GVS induces artificial vestibular signals that influence vestibulo-autonomic pathways associated with motion sickness (Quinn et al., 2015), whereas cathodal tDCS over the TPJ likely exerts a top-down modulatory effect on higher-order vestibular-insular-parietal networks involved in sensory conflict resolution and interoceptive awareness. Although both approaches affect overlapping vestibularrelated circuits, GVS primarily alters vestibular input at the peripheral level, while tDCS modulates cortical processing of multisensory information, which may explain the selective reduction in nausea observed in the present study. Previous tDCS studies have found delayed onset and more rapid recovery of cybersickness symptoms after 15 min of 1.5 mA cathodal tDCS compared to anodal tDCS (Gandiga et al., 2006; Li et al., 2020). Furthermore, our results align with previous findings demonstrating that cathodal tDCS applied to the parietal cortex can mitigate motion sickness induced by rotating chairs. Given that cathodal tDCS is known to inhibit neuronal activity in targeted brain regions, our observations support the hypothesis that direct cortical inhibition may be a key mechanism in reducing cybersickness symptoms (Arshad et al., 2015; Paule et al., 2004). In contrast, anodal tDCS enhances cortical excitability and facilitates adaptive sensory integration processes. It is important to clarify how our study differs from Takeuchi et al.'s work. Takeuchi et al. (2018) applied anodal tDCS before VR exposure and assessed symptoms after VR immersion, demonstrating that anodal tDCS delayed the onset of cybersickness and accelerated recovery, particularly improving oculomotor symptoms. Oculomotor

symptoms in cybersickness include eye strain, difficulty focusing, and blurred vision, reflecting the challenge of maintaining stable gaze, vergence, and accommodation when processing rapidly changing visual stimuli in VR environments. Takeuchi et al. (2018) suggested that anodal tDCS enhanced cortical excitability in the TPJ, thereby facilitating the brain's adaptive capacity to integrate conflicting visual-vestibular information and promoting faster recovery of oculomotor function after VR-induced stress. In contrast, our study applied cathodal tDCS before VR exposure and assessed symptoms immediately after VR immersion. Our findings show that cathodal tDCS directly reduced nausea-related symptoms during sensory conflict processing. These differences suggest complementary mechanisms and clinical applications: anodal tDCS may enhance adaptive mechanisms that facilitate recovery after VR exposure, particularly for oculomotor symptoms, while cathodal tDCS directly reduces cortical responses to sensory conflicts, providing immediate relief of nausea symptoms during or immediately after VR exposure. Nevertheless, disorientation and oculomotor symptoms were not significantly improved by cathodal tDCS in our study. This selective effect on nausea warrants a mechanistic explanation. Different cybersickness symptoms are mediated by distinct neural pathways. Nausea is primarily driven by vestibular-autonomic pathways projecting from the TPJ to brainstem emetic centers, including the area postrema and nucleus tractus solitarius. Cathodal tDCS over the TPJ likely reduced cortical excitability in these vestibular-autonomic projections, thereby attenuating nausea. In contrast, disorientation symptoms arise from spatial orientation processing involving broader networks, including the posterior parietal cortex, retrosplenial cortex, and hippocampus, which extend beyond the TPJ stimulation field. Similarly, oculomotor discomfort reflects eye strain and accommodation demands mediated by frontal eye fields and occipital visual areas, which were not targeted by our stimulation. The insufficient stimulation power to modulate these distributed networks may also have contributed to the lack of effect on disorientation and oculomotor symptoms (Takeuchi et al., 2018). These findings suggest that nausea-related pathways are more focally organized within the TPJ, making them more susceptible to localized neuromodulation than the distributed networks underlying other cybersickness symptoms. Although the sensory conflict theory provides a partial explanation for cybersickness, it does not fully account for all aspects of its occurrence.

In the cathodal tDCS group, our analysis of hemodynamic responses revealed decreased activity in the TPJ, particularly in the superior parietal lobule and angular gyrus. This reduction in activity, indicated by decreased HbO levels, was accompanied by a decrease in cybersickness symptoms. These findings suggest an inhibitory effect of

<sup>\*</sup>p < 0.05.



cathodal tDCS on the targeted brain regions. The TPJ is a large region that includes the superior temporal gyrus, middle temporal gyrus, superior parietal lobule, supramarginal gyrus, angular gyrus, and parietal operculum. This anatomical complexity raises questions about how cathodal tDCS targeting this broad region produces specific effects on cybersickness. However, the TPJ should be understood not as isolated subregions but as an interconnected network for vestibular processing and multisensory integration (Frank and Greenlee, 2018; Dieterich and Brandt, 2008). Previous studies have shown that the TPJ exhibits coordinated activation patterns during sensory conflict conditions, particularly when visual

and vestibular inputs are incongruent (Nguyen et al., 2020). Our findings of decreased activity in both the superior parietal lobule and angular gyrus following cathodal tDCS support this network-level modulation. The observed reduction in cybersickness symptoms likely reflects cumulative effects across multiple TPJ subregions involved in processing conflicting sensory information. This modulation of sensory integration processes may explain the observed reduction in cybersickness symptoms (Dalong et al., 2021). EEG studies during VR immersion have demonstrated that alpha suppression in the temporoparietal lobe is a key indicator of multisensory vestibular cortex activation. This alpha suppression is

typically associated with increased cortical processing of vestibular information. However, our findings suggest that cathodal tDCS may modulate this activity. By potentially reducing alpha suppression, cathodal tDCS could disrupt the normal functioning of the vestibular region. This disruption, in turn, may lead to a reduction in MS symptoms and postural sway as the brain's processing of conflicting sensory information is altered (Gale et al., 2016). Consequently, it was determined that the application of cathodal tDCS showed a decreased effect on cybersickness by inducing changes in the activity of the cerebral cortex related to body and spatial orientation.

The present study demonstrates that cathodal tDCS applied to the right TPJ in healthy adults effectively reduces both cybersickness symptoms and cortical activity induced by VR exposure. In contrast, sham tDCS showed no significant improvements in motion sickness symptoms or changes in cerebral cortical activity following VR exposure. Our between-group analysis corroborates these findings, revealing a significant decrease in cybersickness symptoms associated with the inhibitory effect of cathodal tDCS.

In addition to cortical modulation of visual-vestibular integration, alternative physiological and emotional mechanisms may also contribute to the observed reduction in nausea. tDCS modulates vagal tone and cardiac autonomic activity (Montenegro et al., 2011) and influence interoceptive regions such as the insula that are involved in nausea perception (Napadow et al., 2013). Moreover, limbic system activity related to stress and anxiety may also affect cybersickness severity as emotional arousal and anticipatory stress can amplify symptom perception during VR exposure (Dennison et al., 2016). Although our findings primarily support cortical sensory integration as the main mechanism, partial involvement of autonomic–emetic and limbic–emotional pathways cannot be excluded.

Despite these promising results, several limitations warrant consideration: first, our study did not include follow-up measurements to determine the duration of tDCS aftereffects on cortical activity and cybersickness symptoms. fNIRS and SSQ assessments were performed only immediately after the 20-min stimulation; therefore, the persistence of these effects remains unclear. Second, our sample size was relatively small (N = 10 per group), which limits statistical power and may increase the risk of type II error. The study may have been underpowered to detect smaller but potentially meaningful effects on disorientation and oculomotor symptoms. Future studies with larger sample sizes are needed to confirm our findings and detect more subtle effects. Third, the population consisted of healthy adults in their 20s, potentially limiting the applicability of our findings to other age groups. Fourth, due to methodological issues, we used a discrete cosine transform temporal parameter with a high-pass period cut-off of 128 s, which is comparable to the 120-s task block duration. We acknowledge that this filter setting, with a cut-off period longer than the task duration, may have attenuated or eliminated a portion of the task-related hemodynamic response. This poses a risk of confounding the signal with the noise that the filter was intended to eliminate. Despite this limitation, we were able to detect significant cortical activation patterns and between-group differences, suggesting that meaningful task-related signals were preserved. However, future studies should optimize highpass filter parameters (e.g., using a cut-off period substantially longer than the task duration, such as 200-300 s) to minimize signal attenuation while effectively removing slow drift artifacts. Fifth, in this study, the fNIRS recording regions were limited to the bilateral temporoparietal regions. Further studies investigating the role of the frontal and parietal cortices in sensory conflict are needed. Finally, tDCS delivery regions and stimulation were limited. We suggest that these relationships and differences should be studied using anodal tDCS delivery to the left TPJ region in the future.

#### Conclusion

We demonstrated that cathodal tDCS over the right TPJ induces a more synchronized brain state, potentially suppressing neural networks associated with cybersickness-induced nausea. These findings underscore the critical role of the TPJ in cybersickness and offer new insights into its neural underpinnings. The ability to modulate cybersickness through external brain stimulation has significant implications for both theoretical understanding and practical applications of VR technology. By potentially reducing cybersickness through tDCS-induced modulation of TPJ activity, we may enhance the effectiveness of VR-based treatments and training programs in clinical contexts. As VR technology evolves, neuromodulation techniques, including tDCS, could prove invaluable in maximizing the benefits of this immersive technology across various fields, ultimately improving user experience and expanding VR applications.

# Data availability statement

The datasets presented in this article are not readily available because the datasets generated during this study are not available due to institutional review board restrictions and privacy protection requirements that prohibit data sharing. Requests to access the datasets should be directed to pgy0614@hanmail.net.

# **Ethics statement**

The studies involving humans were approved by the Institutional Review Board of Dankook University, Cheonan, Republic of Korea (IRB approval number: DKU 2023-01-016-001). The studies were conducted in accordance with the local legislation and institutional requirements. The participants provided their written informed consent to participate in this study.

#### **Author contributions**

SHY: Data curation, Project administration, Software, Visualization, Writing – original draft. SSY: Conceptualization, Formal analysis, Methodology, Writing – review and editing. SP: Conceptualization, Funding acquisition, Investigation, Methodology, Writing – original draft, Writing – review and editing.

#### **Funding**

The authors declare that financial support was received for the research and/or publication of this article. This research was

supported by the Basic Science Research Program through the National Research Foundation of Korea (NRF) funded by the Ministry of Education (NRF RS-2023-00252618).

accuracy, including review by the authors wherever possible. If you identify any issues, please contact us.

#### Conflict of interest

The authors declare that the research was conducted in the absence of any commercial or financial relationships that could be construed as a potential conflict of interest.

#### Generative AI statement

The authors declare that no Generative AI was used in the creation of this manuscript.

Any alternative text (alt text) provided alongside figures in this article has been generated by Frontiers with the support of artificial intelligence and reasonable efforts have been made to ensure

#### Publisher's note

All claims expressed in this article are solely those of the authors and do not necessarily represent those of their affiliated organizations, or those of the publisher, the editors and the reviewers. Any product that may be evaluated in this article, or claim that may be made by its manufacturer, is not guaranteed or endorsed by the publisher.

# Supplementary material

The Supplementary Material for this article can be found online at: https://www.frontiersin.org/articles/10.3389/frvir.2025.1688562/full#supplementary-material

## References

Arshad, Q., Cerchiai, N., Goga, U., Nigmatullina, Y., Roberts, R. E., Casani, A. P., et al. (2015). Electrocortical therapy for motion sickness. *Neurology* 85, 1257–1259. doi:10.1212/wpl.0000000000001989

Ayaz, H., Izzetoglu, M., Izzetoglu, K., and Onaral, B. (2019). "The use of functional near-infrared spectroscopy in neuroergonomics," in *Neuroergonomics* (Elsevier), 17–25.

Azhari, A., Bizzego, A., and Esposito, G. (2021). Father-child dyads exhibit unique inter-subject synchronization during co-viewing of animation video stimuli. *Soc. Neurosci.* 16, 522–533. doi:10.1080/17470919.2021.1970016

Bailey, J. O., and Bailenson, J. N. (2017). "Immersive virtual reality and the developing child," in *Cognitive development in digital contexts* (Elsevier), 181–200.

Baker, W. B., Parthasarathy, A. B., Busch, D. R., Mesquita, R. C., Greenberg, J. H., and Yodh, A. (2014). Modified beer-Lambert law for blood flow. *Biomed. Opt. Express* 5, 4053–4075. doi:10.1364/boe.5.004053

Bisdorff, A. (2014). Migraine and dizziness. Curr. Opin. Neurol. 27 (1), 105–110. doi:10.1097/WCO.0000000000000001

Bouchard, S., Robillard, G., and Renaud, P. (2007). Revising the factor structure of the Simulator Sickness Questionnaire. *Annu. Rev. Cyberther. Telemed.* 5, 128–137.

Cesari, V., Gaggero, G., Paladino, M. P., Dellantonio, S., and Chinellato, E. (2024). The effects of right temporoparietal junction stimulation on embodiment, presence, and performance in teleoperation. *AIMS Neurosci.* 11, 352–372. doi:10.3934/Neuroscience.

Cope, M., and Delpy, D. T. (1988). System for long-term measurement of cerebral blood and tissue oxygenation on newborn infants by near infra-red transillumination. *Med. Biol. Eng. Comput.* 26, 289–294. doi:10.1007/bf02447083

Dalong, G., Jiyuan, L., Yubin, Z., Yufei, Q., Jinghua, Y., Cong, W., et al. (2021). Cathodal transcranial direct current stimulation over the right temporoparietal junction suppresses its functional connectivity and reduces contralateral spatial and temporal perception. *Front. Neurosci.* 15, 629331. doi:10.3389/fnins.2021.629331

Dennison, M. S., Wisti, A. Z., and D'Zmura, M. (2016). Use of physiological signals to predict cybersickness. *Displays* 44, 42–52. doi:10.1016/j.displa.2016.07.002

Diemer, J., Alpers, G. W., Peperkorn, H. M., Shiban, Y., and Mühlberger, A. (2015). The impact of perception and presence on emotional reactions: a review of research in virtual reality. *Front. Psychol.* 6, 26. doi:10.3389/fpsyg.2015.00026

Dieterich, M., and Brandt, T. (2008). Functional brain imaging of peripheral and central vestibular disorders. *Brain* 131, 2538–2552. doi:10.1093/brain/awn042

Filmer, H. L., Dux, P. E., and Mattingley, J. B. (2014). Applications of transcranial direct current stimulation for understanding brain function. *Trends Neurosci.* 37, 742–753. doi:10.1016/j.tins.2014.08.003

Flöel, A. (2014). tDCS-enhanced motor and cognitive function in neurological diseases. *NeuroImage* 85, 934–947. doi:10.1016/j.neuroimage.2013.05.098

Frank, S. M., and Greenlee, M. W. (2018). The parieto-insular vestibular cortex in humans: more than a single area? *J. Neurophysiol.* 120, 1438–1450. doi:10.1152/jn. 00907.2017

Gale, S., Prsa, M., Schurger, A., Gay, A., Paillard, A., Herbelin, B., et al. (2016). Oscillatory neural responses evoked by natural vestibular stimuli in humans. *J. Neurophysiol.* 115, 1228–1242. doi:10.1152/jn.00153.2015

Gandiga, P. C., Hummel, F. C., and Cohen, L. G. (2006). Transcranial DC stimulation (tDCS): a tool for double-blind sham-controlled clinical studies in brain stimulation. *Clin. Neurophysiol.* 117, 845–850. doi:10.1016/j.clinph.2005.12.003

Herold, F., Wiegel, P., Scholkmann, F., Müller, N. G., Hamacher, D., and Schega, L. (2017). Functional near-infrared spectroscopy in movement science: a systematic review on cortical activity in postural and walking tasks. *Neurophotonics* 4, 041403. doi:10.1117/1.nph.4.4.041403

Hidalgo-Muñoz, A. R., Mouratille, D., Matton, N., Causse, M., Rouillard, Y., El-Yagoubi, R., et al. (2019). Hemodynamic responses to visual cues during attentive listening in autonomous *versus* manual simulated driving: a pilot study. *Brain Cogn.* 135, 103583. doi:10.1016/j.bandc.2019.103583

Jöbsis, F. F. (1977). Noninvasive, infrared monitoring of cerebral and myocardial oxygen sufficiency and circulatory parameters. *Science* 198, 1264–1267. doi:10.1126/science.929199

Kennedy, R. S., Lane, N. E., Berbaum, K. S., and Lilienthal, M. G. (1993). Simulator sickness questionnaire: an enhanced method for quantifying simulator sickness. *Int. J. Aviat. Psychol.* 3, 203–220. doi:10.1207/s15327108ijap0303\_3

Kheradmand, A., and Winnick, A. (2017). Perception of upright: multisensory convergence and the role of temporo-parietal cortex. *Front. Neurol.* 8, 552. doi:10. 3389/fneur.2017.00552

LaViola, J. J. (2000). A discussion of cybersickness in virtual environments. ACM SIGCHI Bull. 32, 47–56. doi:10.1145/333329.333344

Lefaucheur, J.-P., Antal, A., Ayache, S. S., Benninger, D. H., Brunelin, J., Cogiamanian, F., et al. (2017). Evidence-based guidelines on the therapeutic use of transcranial direct current stimulation (tDCS). *Clin. Neurophysiol.* 128, 56–92. doi:10.1016/j.clinph.2016. 10.087

Li, G., Varela, F. M., Habib, A., Zhang, Q., McGill, M., Brewster, S., et al. (2020). "Exploring the feasibility of mitigating VR-HMD-induced cybersickness using cathodal transcranial direct current stimulation," in 2020 IEEE international conference on artificial intelligence and virtual reality (AIVR) (IEEE), 1–8.

Llorens, R., Fuentes, M. A., Borrego, A., Latorre, J., Alcañiz, M., Colomer, C., et al. (2021). Effectiveness of a combined transcranial direct current stimulation and virtual reality-based intervention on upper limb function in chronic individuals post-stroke with persistent severe hemiparesis: a randomized controlled trial. *J. Neuroeng. Rehabil.* 18, 108. doi:10.1186/s12984-021-00896-2

Montenegro, R. A., Farinatti, P. T., Fontes, E. B., Soares, P. P. d. S., Cunha, F. A. d., Gurgel, J. L., et al. (2011). Transcranial direct current stimulation influences the cardiac autonomic nervous control. *Neurosci. Lett.* 497, 32–36. doi:10.1016/j.neulet.2011.04.019

Napadow, V., Sheehan, J. D., Kim, J., LaCount, L. T., Park, K., Kaptchuk, T. J., et al. (2013). The brain circuitry underlying the temporal evolution of nausea in humans. *Cereb. Cortex* 23, 806–813. doi:10.1093/cercor/bhs073

Nguyen, N. T., Takakura, H., Nishijo, H., Ueda, N., Ito, S., Fujisaka, M., et al. (2020). Cerebral hemodynamic responses to the sensory conflict between visual and rotary vestibular stimuli: an analysis with a multichannel near-infrared spectroscopy (NIRS) system. Front. Hum. Neurosci. 14, 125. doi:10.3389/fnhum.2020.00125

Nitsche, M. A., and Paulus, W. (2001). Sustained excitability elevations induced by transcranial DC motor cortex stimulation in humans. *Neurology* 57, 1899–1901. doi:10. 1212/wnl.57.10.1899

Nitsche, M. A., Cohen, L. G., Wassermann, E. M., Priori, A., Lang, N., Antal, A., et al. (2008). Transcranial direct current stimulation: state of the art 2008. *Brain Stimul.* 1, 206–223. doi:10.1016/j.brs.2008.06.004

Paule, M. G., Chelonis, J. J., Blake, D. J., and Dornhoffer, J. L. (2004). Effects of drug countermeasures for space motion sickness on working memory in humans. *Neurotoxicol. Teratol.* 26, 825–837. doi:10.1016/j.ntt.2004.07.002

Perpetuini, D., Russo, E. F., Cardone, D., Palmieri, R., De Vittorio, M., Rossini, P. M., et al. (2022). Identification of functional cortical plasticity in children with cerebral palsy associated to robotic-assisted gait training: an fNIRS study. *J. Clin. Med.* 11, 6790. doi:10.3390/jcm11226790

Pfeifer, M. D., Scholkmann, F., and Labruyère, R. (2018). Signal processing in functional near-infrared spectroscopy (fNIRS): methodological differences lead to different statistical results. *Front. Hum. Neurosci.* 11, 641. doi:10.3389/fnhum.2017.00641

Pfeiffer, C., Serino, A., and Blanke, O. (2014). The vestibular system: a spatial reference for bodily self-consciousness. *Neurosci* 8, 31. doi:10.3389/fnint.2014.00031

Quinn, V. F., MacDougall, H. G., and Colagiuri, B. (2015). Galvanic vestibular stimulation: a new model of placebo-induced nausea. *J. Psychosom. Res.* 78 (5), 484–488. doi:10.1016/j.jpsychores.2014.12.011

Schmäl, F. (2013). Neuronal mechanisms and the treatment of motion sickness. *Pharmacology* 91, 229–241. doi:10.1159/000350185

Sugiura, A., Tanaka, K., Takada, H., and Miyao, M. (2017). "Effect of difference in information between vision and vestibular labyrinth on a human body," in *Universal access in human-computer interaction designing novel interactions: 11th international conference, UAHCI 2017, held as part of HCI international 2017, Vancouver, BC, Canada, July 9–14, 2017, proceedings, part II 11 (Springer), 652–662.* 

Takeuchi, N., Mori, T., Suzukamo, Y., and Izumi, S.-I. (2018). Modulation of excitability in the temporoparietal junction relieves virtual reality sickness. *Cyberpsychol. Behav. Soc. Netw.* 21, 381–387. doi:10.1089/cyber.2017.0499

Yamamura, H., Baldauf, H., and Kunze, K. (2020). "Pleasant locomotion--towards reducing cybersickness using fNIRS during walking events in VR," in Adjunct proceedings of the 33rd annual ACM symposium on user interface software and technology, 77–79.

Young, S. D., Adelstein, B. D., and Ellis, S. R. (2007). Demand characteristics in assessing motion sickness in a virtual environment: or does taking a motion sickness questionnaire make you sick? *IEEE Trans. Vis. Comput. Graph.* 13, 422–428. doi:10.1109/tvcg.2007.1029

Zhang, D., Zhou, Y., and Yuan, J. (2018). Speech prosodies of different emotional categories activate different brain regions in adult cortex: an fNIRS study. *Sci. Rep.* 8, 218. doi:10.1038/s41598-017-18683-2